Journal of Advanced Research xxx (xxxx) xxx

Contents lists available at ScienceDirect

Journal of Advanced Research

journal homepage: www.elsevier.com/locate/jare

Metabolic responses of sea anemone and jellyfish to temperature and UV bleaching: Insights into stress adaptation using LCMS-based metabolomics, molecular networking and chemometrics

Mohamed A. Farag [a,*,1], Doaa B. Saied [b,1], Sherif M. Afifi [c], Andreas Kunzmann [d], Ludger A. Wessjohann [e], Hildegard Westphal [d,f], Holger Kühnhold [d], Marleen Stuhr [d]

[a] Pharmacognosy Department, Faculty of Pharmacy, Cairo University, Cairo 11562, Egypt
[b] Chemistry Department, School of Sciences and Engineering, The American University in Cairo, New Cairo 11835, Egypt
[c] Department for Life Quality Studies, Rimini Campus, University of Bologna, Corso d'Augusto 237, Rimini 47921, Italy
[d] Leibniz Centre for Tropical Marine Research (ZMT), Fahrenheit Str. 6, Bremen 28359, Germany
[e] Department of Bioorganic Chemistry, Leibniz Institute of Plant Biochemistry (IPB), Weinberg 3, Halle (Saale) 06120, Germany
[f] Department of Geosciences, University of Bremen, Bremen 28359, Germany

ARTICLE INFO

Article history:
Received 7 June 2024
Revised 29 August 2024
Accepted 10 October 2024
Available online xxxx

Keywords:
Entacmaea quadricolor
Cassiopea andromeda
Anemones
Bleaching
Stress
Gnps
Metabolomics

ABSTRACT

Introduction: Climate change poses various threats to marine life, particularly in shallow tropical waters. Objective: The impact of increased temperature and ultraviolet (UV) exposure on two photosymbiotic cnidarians, a common bubble-tip anemone and an upside-down jellyfish, was investigated.
Methods: To illustrate the response of aquatic organisms, the metabolomes of unstressed *Entacmaea quadricolor* and *Cassiopea andromeda* were compared for detailed metabolite profiling. UHPLC-MS coupled with chemometrics and GNPS molecular networking was employed for sample classification and identification of markers unique to stress responses in each organism.
Results: Several compounds with bioactive functions, including peptides and terpenoids, were reported for the first time in both organisms, viz. cyclic tetraglutamate, campestriene, and ceramide aminoethyl phosphonate (CEAP d18:2/16:0). Both anemone and jellyfish were subjected to either elevated UV-B light intensity up to 6.6 KJ m^{-2} or increased temperatures (28 °C, 30 °C, 32 °C, and 34 °C) over 4 days. Phospholipids, steroids, and ceramides emerged as chief markers of both types of stress, as revealed by the multivariate data analysis. Lysophosphatidylcholine (LPC 16:0), LPC (18:0/0:0), and echinoclasterol sulfate appeared as markers in both UV and thermal stress models of the anemone, whereas methyl/propyl cholestane-*hexa*-ol were discriminatory in the UV stress model only. In the case of jellyfish, nonpolar glycosyl ceramide GlcCer (d14:1/28:6) served as a marker for UV stress, whereas polar peptides were elevated in the thermal stress model. Interestingly, both models of jellyfish share a phospholipid, lysophosphatidylethanolamine (LPE 20:4), as a distinctive marker for stress, reported to be associated indirectly with the activity of innate immune response within other photosymbiotic Cnidaria such as corals and appears to be a fundamental stress response in marine organisms.
Conclusion: This study presents several bioinformatic tools for the first time in two cnidarian organisms to provide not only a broader coverage of their metabolome but also broader insights into cnidarian bleaching in response to different stressors, i.e., heat and UV light, by comparing their effects in anemone versus jellyfish.

Introduction

Anemones and jellyfish are aquatic members of the phylum *Cnidaria*, which includes corals and hydroids. Anemones belong to the class Anthozoans, whereas jellyfish belong to the class Scyphozoa. Cnidarians are known for their specialized stinging cells, which contain tiny harpoon-like structures called nematocysts. These nematocysts are used for defence and predation [1].

Entacmaea quadricolor is a species of sea anemone that belongs to the family Actiniidae, also commonly known as the bubble-tip anemone due to the distinctive "bubble-like" appearance of their tentacles. It is known for its mutual symbiotic relationship with

* Corresponding author.
E-mail address: mohamed.farag@pharma.cu.edu.eg (M.A. Farag).
[1] Equal contribution.

https://doi.org/10.1016/j.jare.2024.10.007
2090-1232/

certain species of clownfish [2], particularly those from the genera *Amphiprion* [3] and *Premna*. The latter live within the tentacles of anemones protected against predators and unharmed by the host's nematocytes. It has not been confirmed whether anemones produce a protective mucous coating, or whether the mucous coat prevents nematocyte discharge [4]. *E. quadricolor* has a mid-range haemolytic and neurotoxic toxicity. Furthermore, the bubble-tip anemone forms associations with 16 of the 28 anemonefish species [5]. The bubble-tip anemone has unique tentacle shapes that increase the surface area in which the anemonefish can hide. Therefore, *E. quadricolor* is considered the most popular host of anemonefish, yet research on its venom composition is limited [6]. Anemones provide habitat and sustenance to many marine organisms and are threatened by coral bleaching upon disruption of such a symbiotic relationship. Bleaching occurs when cnidarians lose their vibrant colors and become noticeably clear, opaque, or white because of the absence of their photosymbiotic organisms, i.e., zooxanthellae and other symbiotic algae [7] under stress conditions such as elevated temperatures associated with climate change [8]. Stressors, such as elevated seawater temperatures, pollution, ultraviolet radiation exposure, and ocean acidification, can disrupt this symbiotic relationship [9] and threaten marine life [10]. For example, the sea anemone *Aiptasia pallida* experiences increased zooxanthellae expulsion when exposed to elevated UV-B and temperature [11] and the *E. quadricolor* is known to respond differently to thermal stress, dependong on their phenotype color and hence endosymbiont community composition [12]. For the sea anemone *Anemonia viridis*, a major transcriptomic response to thermal stress was found within 24 h, which returned to baseline after two days [13]. In comparison, UV radiation alone had little effect but potentiated the response to thermal stress if combined, affecting several specific biological pathways involved in the stress response, including mesoglea loosening, cell death, and calcium homeostasis.

Cassiopea andromeda is a species of jellyfish belonging to the family Cassiopeidae, also known as the upside-down jellyfish, as it lives resting with its flattened bell on the sea floor [14]. Like other jellyfish, *C. andromeda* possesses stinging cells called nematocysts, which are needed for animal feeding and defense. Recent studies have also indicated that jellyfish may serve as a valuable source of bioactive compounds *such as* antioxidant peptides [15,16]. As jellyfish populations have increased dramatically in many marine ecosystems, causing detrimental effects on marine life, there has been growing scientific concern regarding the impact of these animals on marine ecosystems [17]. *Cassiopea* spp. occur commonly across a wide range of shallow tropical habitats, and *C. andromeda*, particularly, even made an appearance in non-indigenous habitats raising the need to investigate and mitigate such phenomenon [18]. The effects of elevated temperature and UV-B radiation on jellyfish are complex, including changes in behavior at sublethal temperatures and enhanced performance (ie.e. greater bell pulsation and diameter) under heat exposure, potentially facilitating range expansion [19] to decrease photosynthetic efficiency and generally reduce the ability to thrive induced by both elevated UV-B and temperature [20], inhibited growth, increased aerobic respiration, and altered enzymatic activities under UV exposure [21]. These studies highlight the complex interplay between environmental stressors and cnidarian physiology, emphasizing the need for further research to understand the long-term effects of climate change on these organisms.

Understanding the impact of global warming on cnidarian metabolism and metabolite production can provide insights into these ecological effects and may lead to solutions [17]. Nevertheless, the consequences of climate change on the cnidarian metabolome remain relatively unexplored field [22–24], although several studies have focused on detecting metabolites derived from cnidarians [25,26] and their possible uses in health treatment [27]. For example, several bioactive metabolites have been reported, such as peptides with strong antioxidant potential, such as hydrolyzed collagen, or with cytotoxic potential on cancer cells [28] hence, their medical importance. Among the chemicals reported in jellyfish, fatty acids and lipid derivatives are the major classes of metabolites [29]. Cnidarians reportedly produce noticeably fewer antimicrobial, antibacterial, antifungal, and antiviral macrolides than other aquatic organisms, suggesting that they are less likely to exert antimicrobial actions [30].

The consequences of cnidarian bleaching extend beyond cnidarians themselves, as many marine organisms depend on them for either protection from predators or their role in nutrient cycling in marine ecosystems [2]. As a result of coral bleaching, the entire marine ecosystem can be disrupted, leading to a decline in biodiversity and wide-reaching ecological and economic impacts on coastal communities [4]. The mutualistic association between corals and intracellular, photosynthetic dinoflagellates belonging to the family Symbiodniaceae is crucial for the survival of coral reef ecosystems. These symbionts are physiologically varied and show distinct patterns of environmental and host dispersion according to genetic data [31]. Therefore, a better understanding of the metabolomic responses and potential interactions of host cnidarians and their diverse photosymbiotic partners is crucial.

This study focused on determining the major effects of environmental climatic change on two different aquatic organisms. *E. quadricolor* and *C. andromeda* through two main stressors: elevated temperature and ultraviolet radiation (UV) as a novel approach. In addition to identifying key metabolites that contribute to the ecological health of marine organisms and are biomarkers of environmental stress caused by global warming, this study aids in predicting the impact of the bleaching process in an earlier phase. The results obtained from this study provide a better understanding of the impact of environmental stress, i.e., UV radiation and thermal stress exposure, on these animals at the metabolome level. The study encompassed four different temperatures (28 °C, 30 °C, 32 °C, and 34 °C), or a daily UV-B (285 and 310 nm) radiation dose of 2.2 KJ m^{-2}, at four different time points.

The Global Natural Products Social Molecular Networking (GNPS) platform and chemometric tools were employed to aid peak identification. The novelty of this study is that it integrates all the aforementioned bioinformatic tools for the first time in both marine organisms to provide not only a broader coverage of their metabolome, but also broader comprehensive insights into cnidarian bleaching in response to different stressors, i.e., heat and UV light, by comparing their effects in anemone versus jellyfish.

Materials and methods

Culture of animals

To conduct a comparative study with two cnidaria species, namely a jellyfish (*Cassiopeia andromeda*) and a sea anemone (*Entacmaea quadricolor*), an *ex-situ* experiment was carried out in the marine experimental facilities (MAREE) at the Leibniz Centre for Tropical Marine Research (ZMT), in Bremen, Germany. The stock cultures of these animals have been cultured in aquaria for about ten years under similar conditions, and both species are therefore assumed to contain highly homogeneous photosymbiont communities. Both species host specific clades of dinoflagellate symbionts from the Symbiodiniaceae family. *Cassiopea* predominantly hosts *Symbiodinium* (clade A), while *Entacmaea quadricolor* typically contains symbionts from *Cladocopium* (clade C), though it can harbor multiple clades depending on environmental

conditions [32,33]. All experiments in this study were conducted in accordance with German ethics on animal welfare.

Before the experiment, *C. andromeda* and *E. quadricolor* specimens were reared in aquarium tanks (200 L) connected to an automated water treatment system, and the water was circulated through a biofilter and a protein skimmer (EHEIM, Germany). Following the recirculating water treatment, approximately 25 % of the culture water was exchanged every week to maintain water quality at the highest level. The tanks were filled with artificial seawater (Red Sea Salt, Red Sea Fish, Israel) with water temperature and salinity set at 26 °C and 35 S_A, respectively. The ambient light was provided artificially using Aquaillumination Hydra FiftyTwo HD (AI Hydra 52 HyperDrive, USA) lamps with seven types of LEDs, emitting the full spectrum (380–680 nm) of photoactive radiation (PAR) with a photon flux density of 100 µmol photons m^{-2} s^{-1} under a 12:12 h light/dark cycle. The specimens were fed daily with freshly hatched *Artemia nauplii* and kept under such conditions for at least six months before being used in this study.

Acclimatization and experimental setup

For each species, jellyfish (size from 2 to 6 cm, life span ca. 4 years) and sea anemone (size from 2 to 4 cm, life span ca. 10 years), 48 equally sized (according to wet weight), intact, and healthy individuals were removed from the MAREE baseline tanks and placed into an experimental system. The experimental setup consisted of three water baths (200 L), each containing four plastic aquaria (10 L) carrying eight test organisms (four of each species). In the experimental setup, test specimens were acclimated for one week to baseline salinity (35.0 PSU) and light conditions (blue/white combination of fluorescence bulbs 4×54 W T5 at a 12 h day/night cycle). The temperature was incrementally increased to 28 °C during the acclimatization phase. After this week of acclimatization, an experimental phase with a length of four days was started. Throughout the experimental phase, the water temperature in one water bath was elevated (2 °C/day) to reach 30 °C on day two, 32 °C on day three, and 34 °C on the final day four. In the second water bath, the test specimens were exposed to a daily dose (2.2 KJ m^{-2}) of UV-B (285 and 310 nm) irradiation. The daily UV-B dose was emitted throughout 1 h over the experimental time the specimens received a total UV-B dose of 2.2 KJ m^{-2} on day two, 4.4 KJ m^{-2} on day three, and 6.6 KJ m^{-2} on day four. The third water bath served as a control treatment, with constant environmental parameters set at the end of the acclimatization phase. To maintain good water quality in the closed plastic aquaria, the test specimens were not fed during the acclimatization and experimental phases, and 30 % of the water volume was exchanged daily. To maintain a constant salinity in the aquaria, the volume of evaporated water was refilled daily with osmosis water before water exchange.

In addition to the monitoring of water parameters, the following data collection and sampling routine was conducted daily throughout the experiment: 1) documentation of general vitality parameters for *C. andromeda* (number of bell pulsations per minute) and *E. quadricolor* (organism closed or tentacles spread out) and observations such as behavioral abnormalities and injuries. 2) quantum yield of photosystem II (PSII) (Fv/Fm) using pulse amplitude-modulated fluorometry (Diving-PAM; Walz, Effeltrich, Germany). 3) Sampling one specimen of each species from every plastic aquarium (n = 4) per treatment by snap-freezing the whole specimen in liquid nitrogen and storing it at −80 °C until further chemical analyses.

Chemicals and reagents

LC/MS grade solvents were purchased from Baker (The Netherlands), and MilliQ water was used for all LC analyses. Sarcophine standard was purchased from AG Scientific (San Diego, CA, USA). Louis, MO, USA).

Sample preparation for (UHPLC-ESI-LIT-Orbitrap-MS) analysis

Sample extraction followed the protocol described in a previous report [34] with some modifications explained as follows. Approximately 20 mg of powdered freeze-dried anemone or jellyfish tissues was ground with a pestle in a mortar under liquid nitrogen. The powder was then homogenized with 2.0 mL 100 % ethanol containing 10µg ml^{-1} umbelliferone (as an internal standard for UHPLC-MS) using an ultrasonic bath for 20 min. The extracts were then centrifuged at 12,000×g for 5 min to remove debris. For UHPLC-MS analyses, 500 µL was aliquoted and filtered through a 22 µm filter. For each specimen, four biological replicates were extracted and analyzed in parallel under the same conditions.

Metabolites profiling of animal extracts via high-resolution ultra-high performance liquid chromatography-mass spectrometry analysis (UHPLC-ESI-LIT-Orbitrap-MS)

For metabolite profiling in control and stressed animal specimens at different time points, runs of UHPLC-ESI linear ion trap-orbital trap hybrid mass spectrometry were carried out using a Dionex UltiMate 3000 UHPLC system coupled to an Orbitrap Elite mass spectrometer (Thermo Fisher Scientific, Germany). UHPLC separation was carried out on a Waters Acquity HSS T3 column (particle size 1.8 µm, pore size 100 Å, 100×1 mm ID, Waters GmbH, Eschborn, Germany), column temperature 40 °C using the same binary gradient and flow rate described for the LCQ Deca XP MAX system using water and acetonitrile supplemented with 0.1 % formic acid as eluents A and B, respectively. The flow rate was set at 0.15 mL min^{-1}, and the following separation gradient starting on injection was implemented: 1 min of 5 % B, linear ramp to 100 % B in 10 min, isocratic part at 100 % B for the next 8 min with ramp back to 5 % B in 1 min and a re-equilibration phase of 10 min, with an injection volume of 2 µL. Mass spectra were collected in negative and positive ion modes for the *m/z* range of 200 – 2,000, heated ESI source set at 250 °C, spray voltage 4.0 kV, capillary temperature 300 °C, FTMS resolution 30,000. In the positive and negative modes, the sheath, auxiliary, and sweep gases (nitrogen) were adjusted to 18, 12, and 0 arbitrary units or 20, 5, and 1 arbitrary units, respectively. The CID mass spectra (buffer gas: helium) in the data-dependent acquisition (DDA) mode were recorded using a normalized collision energy of 35 % with an FTMS resolution of 15,000. The data were evaluated using Xcalibur software 2.2 SP1.48.

UHPLC-MS data processing, metabolites identification, and modeling

Raw data were visualized using the open-access data analysis software Mzmine 2.53 [35], where peaks were identified according to their retention times, accurate masses, elution order, fragmentation patterns, and formulas suggested by the software. The files were further analyzed by exporting mgf-files to Sirius 4.9.12 + CSI:FingerID software [36] (https://bio.informatik.uni-jena.de/sirius/) to manually search structural databases, i.e., PubChem, a phytochemical dictionary of natural products, to aid in identifica-

tion, where structural hits search was set to 20 ppm as *m/z* tolerance cut off.

Feature-based molecular networking

The Global Natural Products Social Molecular Networking (GNPS) platform is a powerful database that has revolutionized the identification of metabolites, enabling scientists to explore the immense potential of natural marine products. Compounds are aligned in generated molecular networks that serve as visual representations of the chemical relationships between different compounds [37]. GNPS was employed to aid peak identification by comparing the tandem mass spectrometry (MS/MS) data to online databases and distributing metabolites in classified clusters, especially as the first attempt in both marine organisms.

Raw UHPLC-MS/MS files were uploaded as mgf files to the Global Natural Products Social Molecular Networking open-access website (https://gnps.ucsd.edu). Data were analyzed using an online workflow, where the precursor ion mass tolerance and MS/MS fragment ion tolerance were both set to 0.07 Da. Accordingly, networks were created where the edges had a cosine score >0.7 and more than four matching peaks. Further, the spectra in the network were queried against GNPS spectral databases (NIST13, MassBank, and Respect) and further visualized and analyzed using Cytoscape software.

UHPLC-MS multivariate data analysis

Furthermore, chemometric tools were employed to aid in species classification and marker identification in response to different stressors. Unsupervised principal component analysis (PCA), in addition to supervised methods such as orthogonal projection to least-squares discriminant analysis (OPLS-DA), was employed [10]. The raw files of UHPLC-MS of all samples were converted into ".abf" files, using an ABF converter (https://www.reifycs.com/AbfConverter/). Accordingly, MS-DIAL software (https://prime.psc.riken.jp/compms/msdial/main.html) was employed for data extraction using the following parameters: retention time (0–25 min), mass range (50–1,000 Da), and accurate mass tolerance for MS1 (0.01 Da) and MS2 (0.025 Da). The peak abundance mass list was exported for the multivariate data analysis. The exported data were subjected to unsupervised and supervised multivariate data analysis, i.e., PCA, hierarchical clustering analysis (HCA), and OPLS-DA using SIMCA 14.1 software (Umetrics, Sweden) to show the segregation and aggregation patterns between samples and highlight the variation. All input variables were scaled to the Pareto scale and mean-centered.

Results and Discussion

UV light and thermal impact on cnidarian organisms' appearance and PSII quantum yield

The visual examination of animals during the study of increasing UV light exposure versus increasing tank water temperature from 28 °C to 34 °C over 4 days period revealed how stressors affected the morphological appearance of both organisms. The day 1 samples (Suppl. Fig. 1A) shows anemones and jellyfish under control conditions without UV exposure and at 28 °C. UV-treated anemones sampled on day 2 (2.2 KJ m^{-2}) showed closed tentacles, as depicted in Suppl. Fig. 1B1, while in the case of jellyfish, mucus was discharged, and their tentacles looked centered forming a crown shape Suppl. Fig. 1B2, and some jellyfish lost their tentacles. On the 3rd day of UV exposure (4.4 KJ m^{-2}), jellyfish started to flip over and lose control of their position with more mucus discharge and total loss of tentacles Suppl. Fig. 1(C1, C2). In contrast, the anemones seemed swollen as if they had absorbed an excess of water, showing an oddly translucent appearance, unlike their normal state, and started to turn slightly transparent, as illustrated in Suppl. Fig. 1C3. The elevated temperature did not show obvious morphological differences, except for the sudden death of the anemone on day 4 as the temperature reached 34 °C (Suppl. Fig. 1D1). Conversely, on the 4th day of UV exposure (6.6 KJ m^{-2}), anemones appeared filled with much less water (Suppl. Fig. 1D2, compared to their counterparts under control conditions. In addition, jellyfish showed minimal activity and could not regulate locomotive functions (Suppl. Fig. 1D3).

When exposed to elevated temperature or UV radiation, Fv/Fm declined in anemone reaching minimum value on the 4th and 3rd day, respectively (Suppl. Table 1). Symbionts conferred some tolerance to the host on the first two days, most obvious on the 2nd day. At 32 °C and 34 °C, anemone the thermal tolerance was lost as Fv/Fm declined significantly. In contrast, the decline of Fv/Fm was less pronounced in anemone upon UV exposure suggesting that anemone may differentially acclimate to light levels based on stress phenotype. The jellyfish were more constantly affected by both stressors as manifested in the Fv/Fm decline reaching the lowest value on the 4th day (Suppl. Table 2). In addition, bell pulsations per minute were declined especially upon exposure to UV radiation. Interestingly, Fv/Fm declined faster in anemone compared to jellyfish. This may be attributed to different symbiont genotypes in both animals. Upon exposure to certain stress at the same dose, jellyfish increased their rate of photosynthesis even if PSII damage occurred while, anemone relied on photoinhibition to prevent PSII damage from occurring in the first place [38].

Metabolites profiling in cnidarian organisms via UHPLC-MS aided by molecular networking

To understand the changes in metabolite profiles associated with the bleaching process, alongside anemone and jellyfish metabolome profiles unreported in the literature, untargeted metabolomics in the two cnidarian organisms was attempted via UHPLC-MS in control animals and post-exposure to stressors, i.e., elevated temperature and UV radiation. A total of 134 primary and secondary metabolites were annotated in the control and stressed organisms, as detected in both positive and negative ionization modes, to provide a comprehensive overview of the metabolomes of animals. The identified metabolites were categorized into several classes including phospholipids, glycolipids, fatty acids, peptides, sphingolipids, ceramides, and terpenoids. Metabolite annotation was based on the elution range, i.e., retention time, accurate mass (*m/z*) and molecular formula, tandem MS/MS, and isotopic distribution, as detailed in Suppl. Tables S3 and S4.

Furthermore, global natural product social (GNPS) molecular networking was employed for the first time to aid in the peak identification and annotation of unknown peaks, especially as the first attempt in both species to characterize their metabolome. The relative abundance of each metabolite in different specimens is illustrated in a pie chart for each node, where each sample was encoded with a different color to aid in the visual observation of the segregation patterns (Fig. 1). The colored codes of all samples are explained for each network.

The phospholipid cluster represented the main cluster in both ionization modes, followed by steroids/terpenoids in the negative mode, likely attributed to the improved ionization of terpenoids in the negative ion mode. Ceramides and glycolipid clusters were more detectable in the positive ionization mode, likely because of their nitrogen atoms, especially in ceramides (Figs. 1 and 2 & Suppl. Fig. S2).

GNPS aided in the identification of phospholipid classes based on specific mass losses of 14 and 28 amu at the edges of the clusters, thereby confirming their annotations (Suppl. Fig. S2). This was

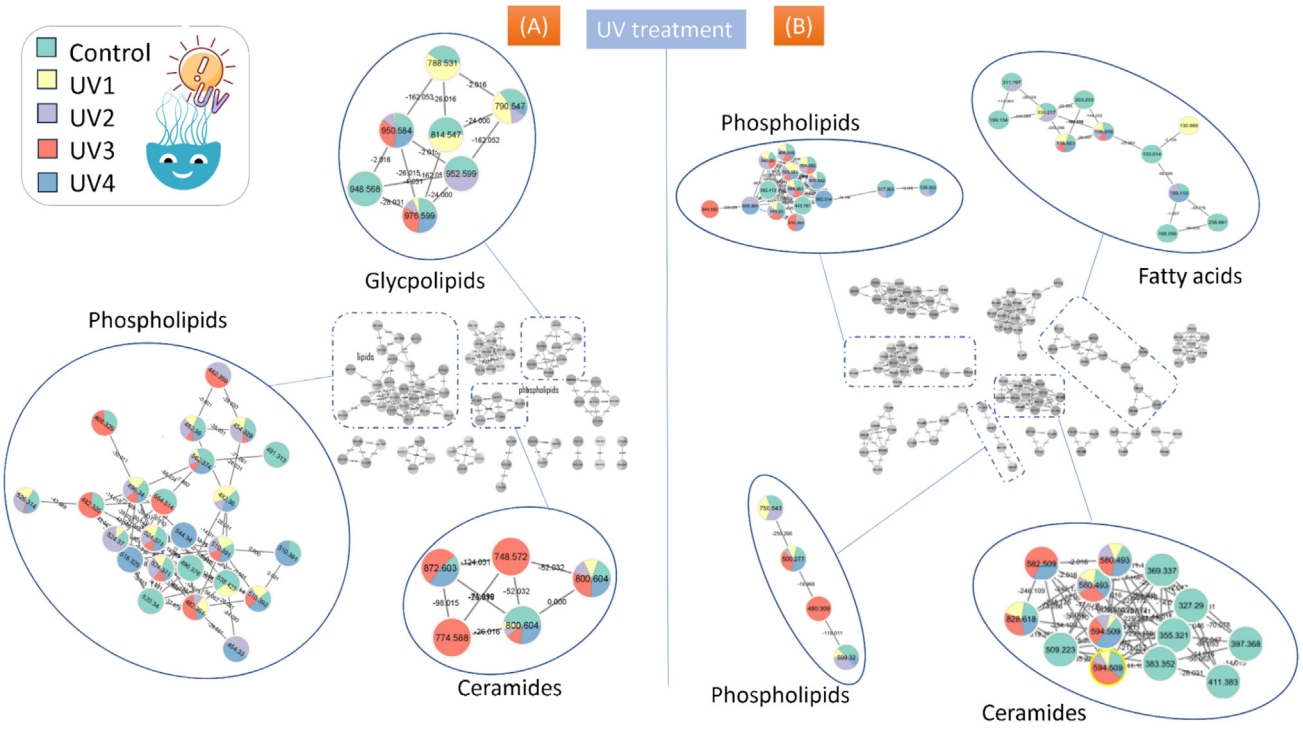

Fig. 1. Molecular networks generated from UHPLC-MS dataset of jellyfish *C. andromeda* after UV exposure; (A) positive ionization mode; and (B) negative ionization mode.

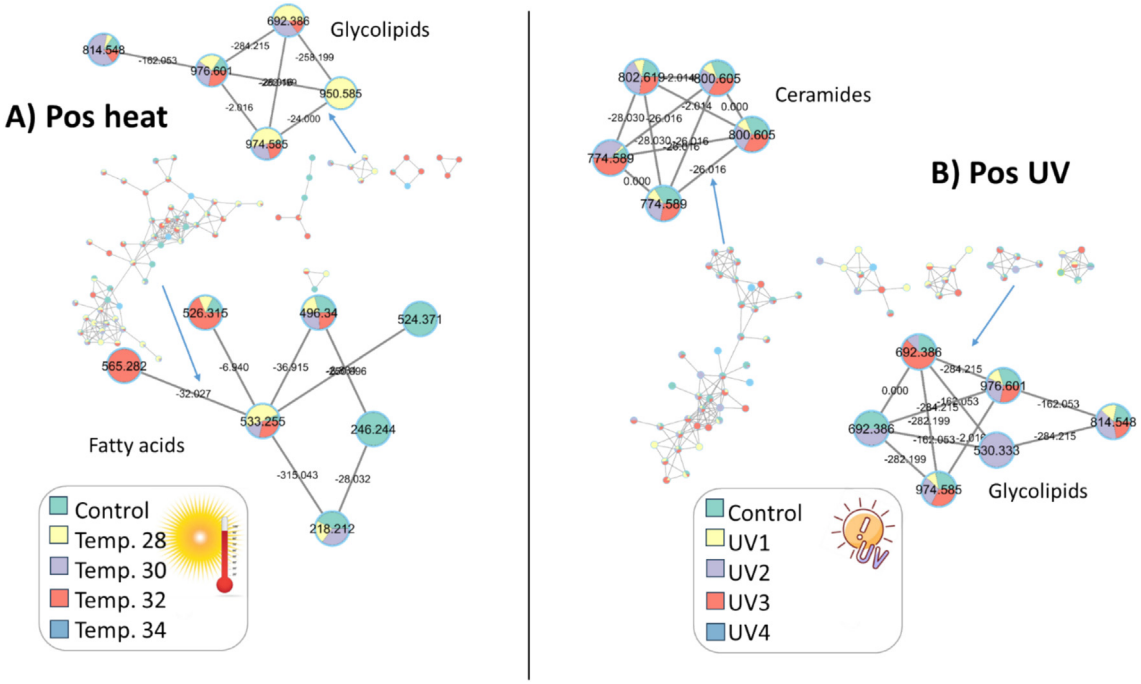

Fig. 2. Molecular networks generated from the UHPLC-MS dataset of anemone *E. quadricolor* showing fatty acids, glycolipids, and ceramide clusters in positive ionization mode, (A) heat stress, and (B) UV stress.

demonstrated in positive ion mode networks, where a node with a precursor mass of *m*/*z* 482 was connected to another node at *m*/*z* 454 through a 28 amu labeled edge, corresponding to the loss of a carbonyl moiety. Likewise, in the negative ion mode network, a tri-nodal cluster built up of precursor masses at *m*/*z* 436, 450, and 464 exhibited 14 and 28 amu labeled edges separating the nodes and corresponding to consecutive demethylation. These mass losses provide valuable insights into the classification and structural characteristics of phospholipids as the major class in both animal species.

Upon manual annotation, nodes with precursor masses of *m*/*z* 950 and *m*/*z* 976 were identified as glycolipids, based on the reported fragmentation [39], and to amount to another major class in both organisms that was detected exclusively in the positive

ionization mode. Subsequently, other members within the same cluster with precursor masses of *m/z* 788, *m/z* 790, *m/z* 814, *m/z* 948, and *m/z* 952 were readily annotated, leveraging the determined class. The presence of edges between these nodes indicates the loss of a hexose moiety (162amu) in certain glycolipids, thereby confirming their annotation (Fig. 2).

Ceramide-related compounds were annotated based on detailed tandem-MS investigation using GNPS-associated libraries. Clusters were built of nodes with mass shifts on the edges of 2 amu (H_2), 14 amu (CH_2), 28 amu (C_2H_4), and 56 amu (C_4H_8) [40]. Ceramide clusters were observed in most networks of jellyfish, regardless of the ionization mode; however, they only appeared in the positive ionized mode networks in the case of anemone. The following subsections explain the identification details for each metabolite class (Suppl. Fig. S3-S9) alongside major changes observed upon exposure to stress conditions in both animals.

Phospholipids (PLs)

Phospholipids (PLs) act as integral membrane components that maintain the integrity of cell membranes [41] and are likely to play a major role in the heat stress response. PLs also contribute to maintaining normal cell physiological functions, such as the production and transport of crucial peptides into the cells of jellyfish [42]. Phospholipids were the most identified metabolite class represented by 21 peaks in *E. quadricolor,* and 25 peaks in *C. andromeda,* with the largest clusters in molecular networks for both positive and negative ionization modes. Phospholipids can be subcategorized into phosphatidylethanolamine (PE), phosphatidylcholine (PC), phosphatidylinositol (PI), lysophospholipids (LP), and lysophosphatidylethanolamine (LPE).

GNPS aided in the identification of phospholipid classes based on specific mass differences of 12 amu, 16 amu, and 28 amu. This was demonstrated in the negative mode networks of anemone, where a node with a precursor mass of *m/z* 478 was connected to three nodes at *m/z* 466, 494, and 450 through 12, 16, and 28-amu labeled edges, respectively (Suppl. Fig. S2a and b). Likewise, a tetra-nodal cluster built up of precursor masses at *m/z* 480 (peak A34), 498 (peak A7), 500 (peak A11), and 522 (peak A47) exhibited 18, 20, 22, and 24 amu labeled edges separating the nodes (Suppl. Fig. S2b). These peaks were annotated as LPE (18:0), PE (O-20:5/0:0), LPE (20:4), and PC (O-18:0/O-1:0).

Additionally, a parent ion at *m/z* 464 with the molecular formula $[C_{23}H_{47}NO_6P]^-$ in peak A39 showed fragmented ions at *m/z* 421 and 267 due to the successive loss of ethyl amine and glycerophosphate moieties, respectively (Suppl. Fig. S3).

In jellyfish, lysophosphatidylcholines (LPCs) were identified mostly based on fragment ion at *m/z* 184 [43], exemplified in LPC (O-16:0) at *m/z* 482 $[M + H]^+$ ($C_{24}H_{53}NO_6P^+$), and LPC (O-14:0) at *m/z* 454 $[M + H]^+$ ($C_{22}H_{49}NO_6P^+$). LPC appeared to decline upon both thermal and UV exposure, thus affecting the cell membrane integrity, which might lead to component diffusion. PEs were mostly detected in the negative ionization mode (Fig. 1B, Suppl. Fig. S2) and identified based on the product ions at *m/z* 140 and 196 (from $[M-H]^-$). Saturated PLs were exemplified in PE (P-16:0) detected at *m/z* 436 ($C_{21}H_{43}NO_6P^-$) and PE (O-18:0) at *m/z* 464 ($C_{23}H_{47}NO_6P^-$) as the major peaks in jellyfish. Polyunsaturated PEs, i.e., LPE (20:4) at *m/z* 500 ($C_{25}H_{43}NO_7P^-$), showed a 1.4-fold increase upon thermal and UV stresses, and opposite to the observed pattern in the case of LPC. Additionally, lysophosphatidylinositol (LPI 18:0) at *m/z* 599 ($C_{27}H_{52}O_{12}P^-$) was annotated based on the fragment ion at *m/z* 241 ($C_6H_{10}O_8P^-$) [44], whereas phosphatidylserine (PS 18:0/0:0) at *m/z* 526 was annotated based on the loss of 87 amu corresponding to the serine group, in accordance with literature [43].

Glycolipids

Glycolipids function as receptors on cell membranes and may account for specific cellular contacts and signal transduction. They have been reported in jellyfish-associated organisms [45] exemplified in monogalactosyldiacylglycerol (MGDG) and digalactosyldiacylglycerol (DGDG). A total of seven peaks were detected in jellyfish, compared to four from this class in anemone (Suppl. Table S3 and S4).

MGDG was annotated based on the typical fragmentation pattern in glycolipids resulting from the combined loss of ammonia NH_3 (17amu), followed by a hexose moiety loss (162amu) leading to an $[M + H\text{-}179]^+$ fragment ion, and the other fragment ion corresponding to $[M + H\text{-}197]^+$, which is formed by the combined loss of NH_3 (17amu) followed by a hexose ring loss (180amu) [39]. MGDG was exemplified in MGDG (38:9) at *m/z* 814 ($C_{47}H_{76}NO_{10}^+$), and MGDG (36:7) at *m/z* 790 ($C_{45}H_{76}NO_{10}^+$). All the identified MGDGs showed a massive decline upon exposure to UV and heat.

Similarly, DGDGs represented in DGDG (36:8) at *m/z* 950 ($C_{51}H_{84}NO_{15}^+$) and DGDG 38:9 at *m/z* 976 ($C_{53}H_{86}NO_{15}^+$) were identified according to reported fragmentation, showing key fragment ions $[M + H\text{-}197]^+$ and $[M + H\text{-}359]^+$ [39]. Both MGDG and DGDG showed an approximately 1.4-to 1.8-fold increase in abundance after thermal exposure.

Sphingolipids/ceramides

Ceramide clusters were observed in positive ion mode with mass shifts on the edges of 2 (H_2), 26 (C_2H_2), and 28 (CO_2) amu (Fig. 2b). Aquatic organisms such as cnidaria (i.e., jellyfish and anemones) are characterized by the presence of sphingophospholipids, which contribute to cellular membrane protection and signaling [46]. In contrast to the aforementioned glycolipids, ceramides are correlated with cold acclimation by increasing unsaturated fatty acid levels in cold habitats [46]. Both organisms encompassed similar numbers of peaks in this class.

In anemone, peak A67 $[M + H]^+$ was detected at *m/z* 554 with a base peak at *m/z* 494 corresponding to the loss of water and propyl groups, in addition to the key fragment ion at *m/z* 146 attributed to the *glycero*-amide unit (Suppl. Fig. S4) and annotated as Cer (t18:0/16:0) (Suppl. Table S3).

In both organisms, ceramide aminoethylphosphonate (CAEP d18:2/16:0) was detected in peak A27 and as regioisomer peaks J23 and J38 at *m/z* 643 $[M + H]^+$, with $C_{36}H_{72}N_2O_5P^+$ as a major peak and annotated with a neutral loss of 125 amu, corresponding to the aminoethylphosphonate moiety [43]. Additionally, glucosylceramide (GlcCer d14:1/28:6) was annotated at *m/z* 800 $[M + H]^+$ and $C_{48}H_{82}NO_8^+$ upon neutral loss of 162 amu and 180 amu [43]. Most ceramides showed increased levels in both treatments, ranging from 1.3 to 3 fold increase.

Peptides

Compared to the abundance of lipid classes in jellyfish, polar cyclic peptides have been detected in both organisms despite the difficulty in their identification due to their low abundance [1]. There is increasing interest in marine peptide characterization owing to their biological activities such as antimicrobial, antitumor, and antiviral properties [47]. It should be noted that in both organisms, peptides were only detected in the negative ionization mode, highlighting the value of comparing the results from both ionization modes.

The molecular ion peak at *m/z* 582 was identified as tuftsin-hexylamide (peak A48), identified in the anemone, showing a base

peak at *m/z* 522, corresponding to the loss of NH_2 and CH_3-CHOH groups (Suppl. Fig. S5).

Cyclic tetraglutamate ($C_{20}H_{27}N_4O_{12}^-$), also known as cnidarin peptide, at *m/z* 515 [48] was detected in *C. andromeda,* which was previously reported in the class *Cubozoa,* known as box jellyfish. Identification was based on the consecutive loss of the glutamyl fragment (129amu), and the appearance of fragment ions at *m/z* 386 $[M-129]^-$ and *m/z* 257 $[M-129-129]^-$. Additionally, the loss of 62 amu in peak J5 confirmed the peptide structure, which summed up the loss of water (18amu), followed by C_2H_4O loss (44amu). Cyclo(isoleucylprolylleucylprolyl) ($C_{22}H_{35}N_4O_4^-$) at *m/z* 419 was previously reported in a jellyfish-associated microbiome [49] and its biosynthesis should be examined to identify the role of the symbiont and/or host in its production.

Terpenoids/steroids

Terpenoids, a major secondary metabolite class in marine organisms, play major ecological roles and are abundantly produced by cnidarians [50], in addition to their several health benefits in humans [51]. The number of identified peaks was slightly higher in anemones (13peaks) than in jellyfish (11peaks) (**Suppl. Table S3 and S4**). They can serve as chemical defence compounds, enhance microbial attachment, and promote symbiosis among different organisms [52]. An algal-associated terpenoid was detected at *m/z* 498 (peak J10) $[M-H]^-$ $(C_{30}H_{44}NO_5)^-$ annotated as the symbiotic terpenoid zooxanthellamine [53], which decreased upon exposure to both stressors. Zooxanthellae algae live within cnidarian tissue, providing the host with energy through photosynthesis [10]. This symbiotic relationship is disrupted in cnidarians during thermal stress [54] and thus likely accounts for the decline in zooxanthellamine levels observed here.

A bisabolene terpenoid (peak J19), previously reported in soft corals [55], another cnidarian, was detected at *m/z* 203 $[M+H]^+$ $(C_{15}H_{23})^+$. Peak A23 in the anemone exhibited a molecular ion at *m/z* 487 and a fragment ion at *m/z* 395, corresponding to the respective loss of ring A and $2H_2$, forming two double bonds. The major fragment ion at *m/z* 377 was attributed to the loss of the side chain attached to C_{13} and two water molecules (Suppl. Fig. S6). Therefore, peak A23 was annotated as methyl cholestadiene tetrol acetate. The molecular ion at *m/z* 327 $[M-H]^-$of peak A45 yielded daughter ions at *m/z* 283, 229, and 191, respectively. The fragment ion at *m/z* 229 was attributed to the loss of acetate and the C_7-C_8 unit (Suppl. Fig. S7), whereas the fission between C_6-C_7 and C_1-C_{14} yielded a daughter ion at *m/z* 191. Hence, peak A45 was annotated as brassicolene [56]. Brassicolene, a cytotoxic diterpenoid, has demonstrated efficacy against lung adenocarcinoma and lymphoma [57], and this is the first time it has been identified in anemones.

Campestadiene (peak J62) was detected in jellyfish, while other steroids exemplified in campestriene (peaks A64, J57) were found in both organisms and annotated based on literature data [58] at *m/z* 383, and *m/z* 381 with proposed formulas $[M+H]^+$ $(C_{28}H_{47})^+$, and $(C_{28}H_{45})^+$, respectively. To the best of our knowledge, this is the first report of all detected terpenoids in jellyfish, and their importance has yet to be examined based on extensive metabolite profiling.

Polyketides (macrolides)

Macrolides are a subclass of natural compounds, known as polyketides. Six peaks were identified in the anemone, compared to only two peaks in the jellyfish. Macrolides are well-known pharmaceuticals with antimicrobial, antibacterial, antifungal, and antiviral activities [30]. Cytotoxicity is the most significant property [59], adding to the potential of these animals as a source of drugs. Peak A5, assigned to salarin B, exhibited $[M-H]^-$ at *m/z* 719 and a base peak at *m/z* 673 owing to the loss of methyl and methoxy groups. Furthermore, the fragment ion at *m/z* 415 was due to cleavage at the ester group (C_1) and alkyl bond at C_{10}-C_{11} in addition to the loss of an acetyl group. In contrast, the fragment ion at *m/z* 397 was attributed to the cleavage of the amide bond (C_7), C_{11}-C_{12}, and C_{16}-C_{17} (Suppl. Fig. S8). Macrolides increased from 1.3 to double folds to both stressors, suggesting their role in stress mitigation.

UHPLC-MS multivariate data analysis (MVA) in response to thermal and UV stress

To assess changes in the anemone and jellyfish metabolome after thermal and UV exposure for marker identification using the UHPLC-MS dataset, a PCA model was constructed in an unsupervised manner. Furthermore, supervised orthogonal partial least squares (OPLS-DA) was employed in cases where PCA failed to predict the markers. The OPLS-DA model was assessed by R^2 and Q^2 values, indicating the model fit and predictability degree, respectively, to avoid model overfit.

Multivariate data analysis of anemone E. quadricolor UHPLC-MS dataset

Unsupervised PCA of the whole E. quadricolor UHPLC-MS dataset post-thermal and UV stress

PCA modeling of the datasets of the anemone *E. quadricolor* showed low total variance coverage in both the negative and positive modes along PC1 and PC2, with a total coverage of 51.7 % in the positive mode model versus 39.8 % in the negative mode model (Suppl. Fig. 10A). The negative mode-based model revealed that phosphatidylethanolamine (PE O-18:0/0:0) was the most distinct biomarker for heat stress based on loading plots (Suppl. Fig. 10B), whereas other markers such as peptides, i.e., seongsanamide A and tuftsin-hexylamide, were less distinctive markers. Markers revealed from the positive ionization mode included LPC (18:0/0:0) and LPC (16:0) as the most discriminating markers, followed by steroids, i.e., methylcholestane-hexaol (peak A20) and propyl-cholesta-hexaol (peak A42) [60] under both heat and UV stress. Hierarchical cluster analysis (Suppl. Fig. 10C) in negative mode showed three main clusters, with the highest temperature (34 °C) and longest UV exposure period (day 4) clustered together in the same subdivision, elaborating the comparable effect on the anemone metabolome and likely to represent extreme stress conditions at all time points.

Unsupervised PCA of E. quadricolor dataset post UV stress

For better marker identification of each stressor effect, PCA models were constructed for UV and thermal stress separately. PCA models of both ionization modes (positive and negative) exhibited a total variance coverage of 64.2 % and 48 %, respectively, higher than the combined PCA of both stressors (Suppl. Fig. 10). The most discriminating metabolites in the UV exposure treatment in the positive ionization mode belonged to lysophospholipids, i.e., LPC (18:0/0:0) and LPC (16:0), followed by steroids, i.e., methylcholestane-*hexa*-ol (peak A20) and propylcholesta-*hexa*-ol (peak A42) (Fig. 3B). In contrast, in the negative ionization mode, phospholipids were the main biomarkers of UV stress, represented by PE (O-18:0/0:0), PE (O-20:0/0:0), PI (18:0/0:0), and PC (O-16:1/0:0) (Fig. 3D).

The detection of phosphatidylcholine in positive ionization mode is enhanced, as these lipids tend to yield abundant protonated molecular ions $[M+H]^+$, while phosphatidylethanolamines detection is enhanced in negative ionization mode, where deprotonated molecular ions $[M-H]^-$ are more prevalent [61]. This dual

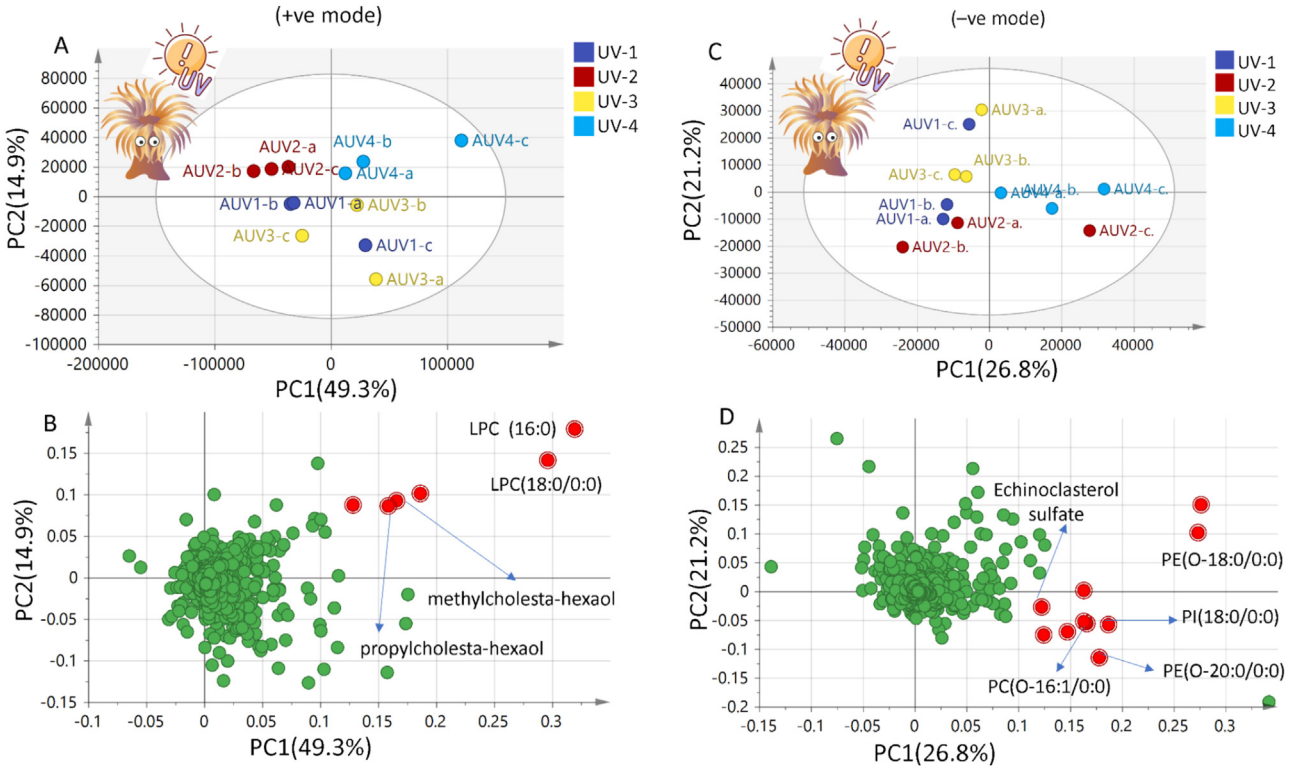

Fig. 3. (A) UHPLC-MS-based PCA score plot model of anemone *E. quadricolor* prescribed by PC1 against PC2 after UV treatment in positive (A) and negative (C) ionization modes. Loading plot for PC1 and PC2 contributing metabolites and their identification in the positive (B) and negative (D) ionization modes.

approach ensures comprehensive coverage and enhanced sensitivity for diverse lipid species in marine samples, and underscores the importance of employing both ionization modes in lipid analysis and stress response monitoring.

Supervised OPLS-DA of E. quadricolor dataset post UV stress

OPLS-DA was employed for modeling the anemone dataset after UV exposure for four consecutive days in the negative ion mode in a supervised mode to aid in biomarker identification and to confirm the results derived from the PCA model. Fig. 4 shows the segregation of the first three days in one class group versus the last day. As expected, high variance coverage and improved prediction power were observed in positive ionization mode (R^2 = 0.99, Q^2 = 0.78, p-value = 0.12; Fig. 4A). The model's S-plot (Fig. 4B), which coincided with the PCA results in the identification of LPC (18:0/0:0) and LPC (16:0) as markers for UV stress, although with a non-significant p-value (approximately 0.12).

Similarly, in the negative ionization mode (Fig. 4D), which was consistent with the PCA results (Suppl. Fig. 10), revealing PE (O-18:0/0:0) and PE (O-20:0/0:0) as markers, yet preceded by PE (O-18:1/0:0) as the most discriminating marker, with a high variance coverage (R^2 = 0.998), prediction power of Q^2 = 0.71, and p-value = 0.23.

A wide range of ecological and biological processes in coral species has been attributed to phospholipids, suggesting their vital value as markers and indicators in coral studies [62],i.e., coral symbiosis [63]. PLs play a crucial role in maintaining membrane structural integrity and creating a selective barrier between cells and the environment that prevents leakage of cellular components. Moreover, they are involved in signaling pathways that respond to stress, including bleaching [64] and the effect of UV exposure on anemones.

Unsupervised PCA of anemone E. quadricolor UHPLC-MS dataset post-thermal stress

To reveal differential metabolites as markers of post-thermal exposure at four different temperatures and for improved discrimination, PCA was modeled separately for this stressor. The score plot revealed segregation of the highest temperature (34 °C) group, with a total variance coverage of 65.4 % (Fig. 5A), and 49.2 % (Fig. 5C) for the positive and negative modes, respectively. Among the markers revealed, phospholipids were the dominant class discriminating the thermal stress effect, i.e. PE (O-18:1/0:0), LPC (16:0), LPC (18:0/0:0), PE (O-20:0/0:0), and PI (18:0/0:0) (Fig. 5B and D). The observed lyso-lipid buildup could potentially represent an independent mechanism contributing to the ability of coral-symbiotic dinoflagellates to withstand heat stress [65]. In addition to lyso-lipids, other markers belonging to peptides (tuftsin-hexylamide) and steroids (methylcholestane-hexaol) (Fig. 5B and D). An unknown metabolite at *m/z* 666 was the most distinctive compound because of the high thermal exposure at 34 °C.

Supervised OPLS-DA of anemone E. quadricolor UHPLC-MS dataset post-thermal stress

Similar to the heat stress exposure PCA model of the anemone, an OPLS-DA approach was employed for the highest temperature (34 °C) modeled in one class at lower temperatures, demonstrating a high total variance coverage R^2 of 95.2 % (positive mode) and 99 % (negative mode), with acceptable prediction powers of Q^2 = 0.85 (positive mode) and 0.81 (negative mode). The generated S-plot

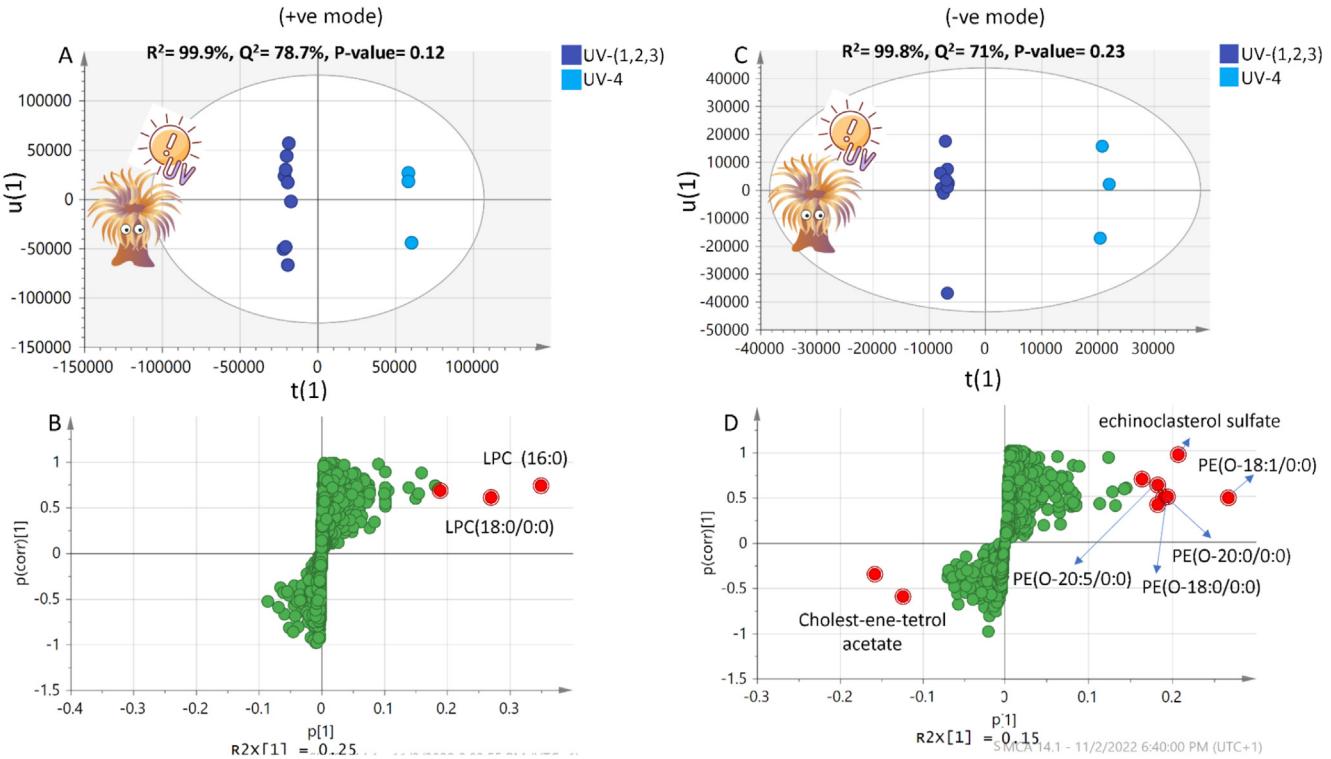

Fig. 4. UHPLC-MS based OPLS-DA score plot of anemone *E. quadricolor* of dataset post UV treatment in positive (A) and negative (C) ionization modes. S-loading plot for contributing metabolites and their identification in positive (B) and negative (D) ionization modes.

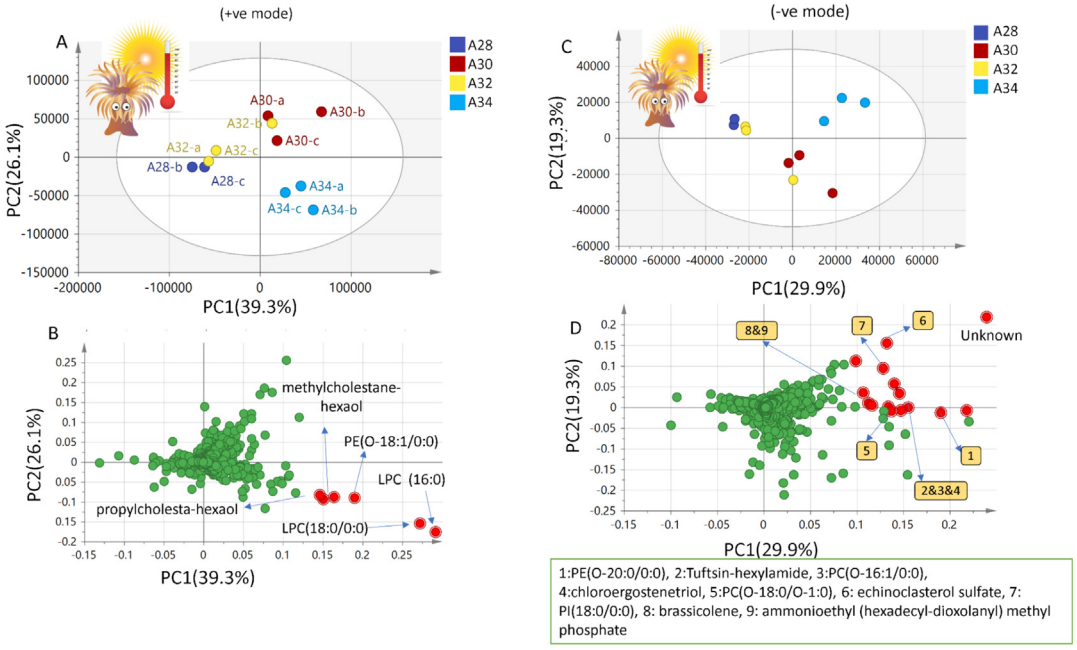

Fig. 5. UHPLC-MS-based PCA score plot model of anemone *E. quadricolor* metabolites analyzed in PC1 versus PC2 of the dataset resulting from thermal treatment in positive (A) and negative (C) ionization modes. Loading plots for PC1 and PC2 contributing metabolites and heat stress markers and their identification in positive (B) and negative (D) ionization modes.

confirmed that LPC (18:0/0:0), and LPC (16:0) belonging to lysophopholipids were the differential metabolites to increase with heat exposure in the positive mode model (Fig. 6B), with a significant p-value of 0.012. In the negative ionization mode, PE (O-20:0/0:0), PI (18:0/0:0), and PC (O-16:1/0:0), which belong to phospholipids, and other markers, i.e., steroid (echinoclasterol sulfate), were revealed as significant (p-value = 0.038, Fig. 6D), highlighting the stronger classification potential in OPLS modeling [66].

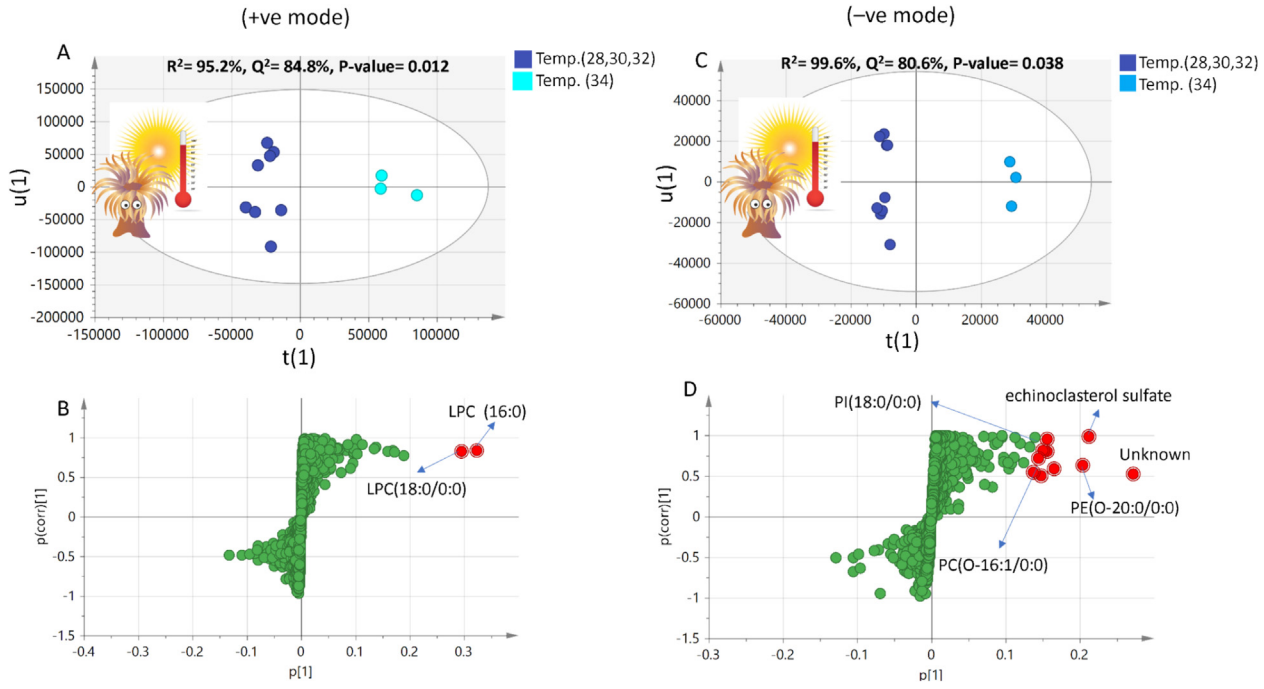

Fig. 6. UHPLC-MS-based OPLS-DA score plot model of anemone *E. quadricolor* dataset resulting from thermal treatment in the positive (A) and negative (C) ionization modes. S-chart for contributing metabolites and their identification in positive (B) and negative (D) ionization modes.

Multivariate data analysis of the jellyfish C. andromeda UHPLC-MS dataset post heat and UV stress

Unsupervised PCA of C. andromeda dataset post-thermal and UV stress

We attempted to compare the modeling results of the anemone with those of the jellyfish to assess whether similar metabolic responses occur in these two organisms. PCA datasets of jellyfish showed low variance coverage in both negative and positive modes along PC1 and PC2 at 40.4 % (Fig. 7A), and 45.7 % (Fig. 7C), respectively. The model revealed that lysophosphatidylethanolamine (LPE 20:4) was the main marker of UV stress, based on the corresponding loading plot (Fig. 7B), whereas glucosylceramide (GlcCer d14:1/28:6) appeared to be the most discriminating marker after heat stress exposure (Fig. 7D).

Unsupervised PCA of C. andromeda dataset post UV stress

For better marker identification of each stressor effect alone, PCA models were employed for UV and thermal stress individually in the jellyfish dataset.

The most discriminating metabolite due to UV exposure in negative ion mode was LPE (20:4). In control samples without UV exposure, the presence of phosphatidylserine (PS 18:0/0:0) was distinctive (Fig. 8). GlcCer (d14:1/28:6) was identified as a marker for UV exposure in positive ionization mode, in addition to LPE (20:4) and an unknown terpenoid at *m/z* 553. Both the negative and positive mode models showed a low total variance coverage of 51.8 % and 57.9 %, respectively. Terpenoids were distinctive for this model and comparable to steroids in the anemone PCA model (Fig. 3).

Supervised OPLS-DA of C. andromeda dataset post UV stress

OPLS was employed for modeling the dataset after UV exposure for four consecutive days in the negative mode, in which the first two days were classified as one class group versus the last two days, based on PCA results (Fig. 8). As expected, a high variance coverage and improved prediction power were observed (R^2 = 0.976, Q^2 = 0.784). The S-plot of the model coincided with the PCA results in the assignment of LPE (20:4) as a marker of UV stress, with a significant p-value of 0.02 (Suppl. Fig. S11). The emergence of unsaturated LPE (20:4) as a marker draws attention to the defense mechanism adapted by jellyfish to maintain their membrane viscosity, as the degree of unsaturation has a direct impact on the vital fluidity of cell membranes [67]. In contrast to the reaction with increased PCs and PEs noted in anemones (Fig. 4), this response lacks the unsaturation observed in jellyfish, and may be suggestive of a differential mechanism to adapt/withstand elevated UV exposure in these animals.

Although the positive ionization mode OPLS results coincided with the PCA results and showed GlcCer d14:1/28:6 as a marker with a total high variance coverage (R^2 = 0.994) and prediction power of Q^2 = 0.755, the model showed a non-significant p-value of 0.26, suggesting that the –ve model was more powerful for elucidating the UV effect on the jellyfish mtabolome, which is likely attributed to improved ionization and detection of this lipid class in the negative ionization mode [61].

Unsupervised PCA of C. andromeda dataset post-thermal stress

To reveal differential metabolites as markers post-thermal exposure at four different temperatures and for improved discrimination, a PCA was modeled separately for the thermal effect. Unlike the clear separation of the highest temperature of 34 °C from other temperature points in the anemone model (Fig. 5), the score plot revealed segregation of the higher 2 temperatures (32 °C and 34 °C), with coverage for PC1 and PC2 at 54.9 % (Suppl. Fig. S12A). The loading plot revealed several new markers at both high and control temperatures (Suppl. Fig. S12B). Phospholipids were the dominant metabolites discriminating the control temperature treatment, i.e., LPI (18:0), LPE (18:0), LPC (18:0), and PS (18:0/0:0). Such markers can be used as predictive monitors for stress in jellyfish, as their decline or disappearance can indicate stressful conditions. Specifically, PS (18:0/0:0) appeared in the thermal and UV models as an early marker of both stressors (Fig. 8). In contrast, thermally stressed jellyfish showed an abundance of LPE (20:4) as a distinctive marker for stress, which was

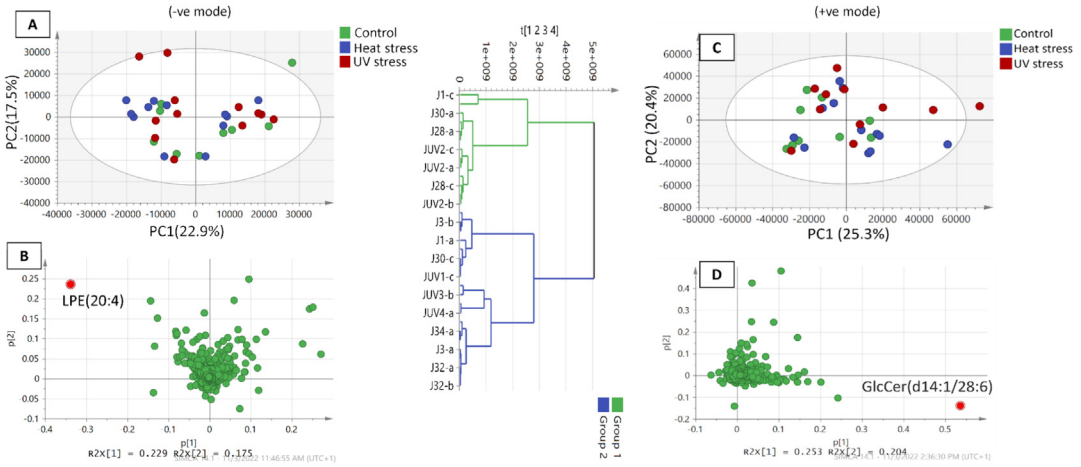

Fig. 7. UHPLC-MS-based PCA score plot model of jellyfish *C. andromeda* metabolites analyzed in PC1 versus PC2 for all datasets analyzed in negative (A) and positive (C) ionization modes. Loading plot for PC1 and PC2 contributing metabolites and their identification in negative (B) and positive (D) ionization modes.

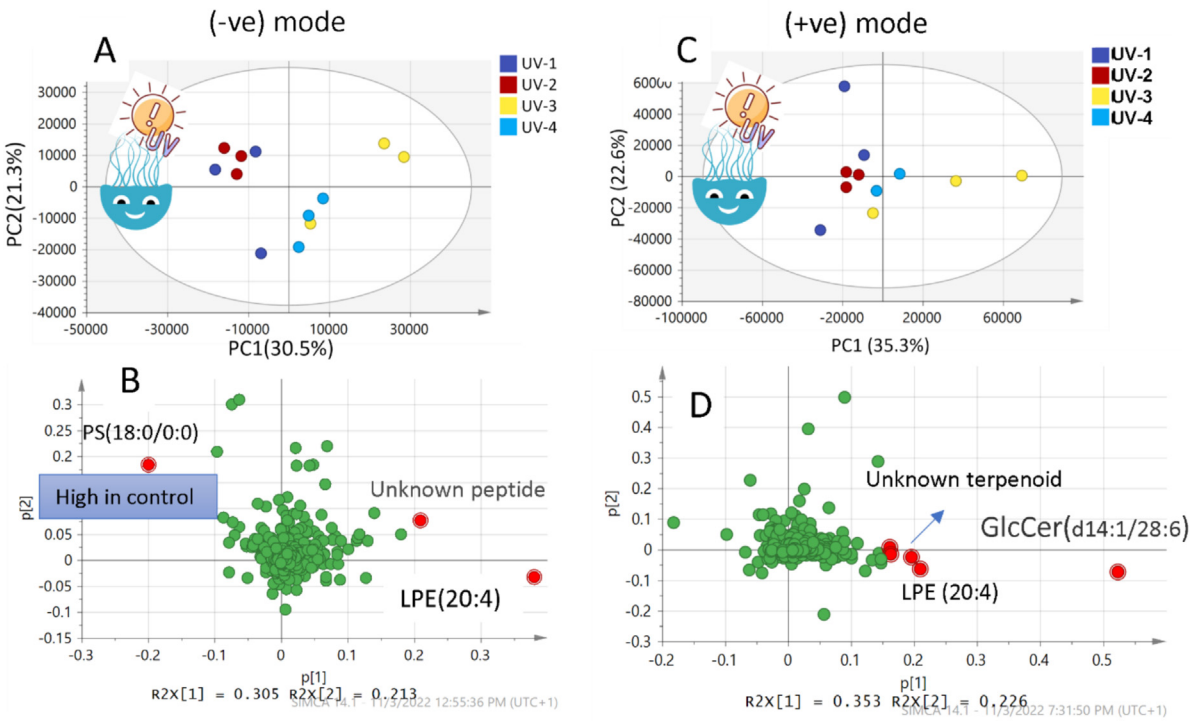

Fig. 8. UHPLC-MS-based PCA score plot model of jellyfish *C. andromeda* metabolites analyzed in PC1 versus PC2 of the dataset resulting from UV treatment in negative (A) and positive (C) ionization modes. Loading plot for PC1 & PC2 contributing metabolites and their identifications in negative (B), and positive (D) ionization modes.

reported to be indirectly associated with the activity of the innate immune system and/or a stress response [68], along with two unknown peptides at *m/z* 433 and *m/z* 977 revealed from the corresponding loading plot (Suppl. Fig. S12B). Marine peptides play vital bioregulatory roles in addressing heat stress by preserving cell integrity, antioxidative potential, and controlling stress hormone levels [69]. Thermal stress caused a noticeable shift in both the nonpolar metabolome pool (as in LPE 20:4) and the polar pool, as well represented by these peptides.

Supervised OPLS-DA of C. andromeda dataset post-thermal stress

Similar to the thermal stress exposure PCA model, an OPLS-DA model was employed for the highest temperature (34 °C), modeled against all other temperatures (Suppl. Fig. S13A), demonstrating a much higher total variance coverage of 99 % (R^2 = 0.99) and a moderate prediction power of Q^2 = 0.75 than that observed in the PCA. The generated S-plot (Suppl. Fig. S13B) confirmed that LPE (20:4), a differential metabolite, increased with thermal stress exposure, which underscores the defense strategy employed by jellyfish to regulate membrane viscosity [67]. The degree of unsaturation plays a crucial role in determining cell membrane fluidity, which is indirectly linked to the activity of the innate immune system and/or stress responses [68]. However, this model showed a non-significant p-value of 0.5 and poor permutation performance with a positive Q^2 value, suggestive of a model overfit, and that the thermal stress response was less observed in the jellyfish than in the anemone. This may be attributed to different algal symbiont clades or strains in animals with different environmental preferences.

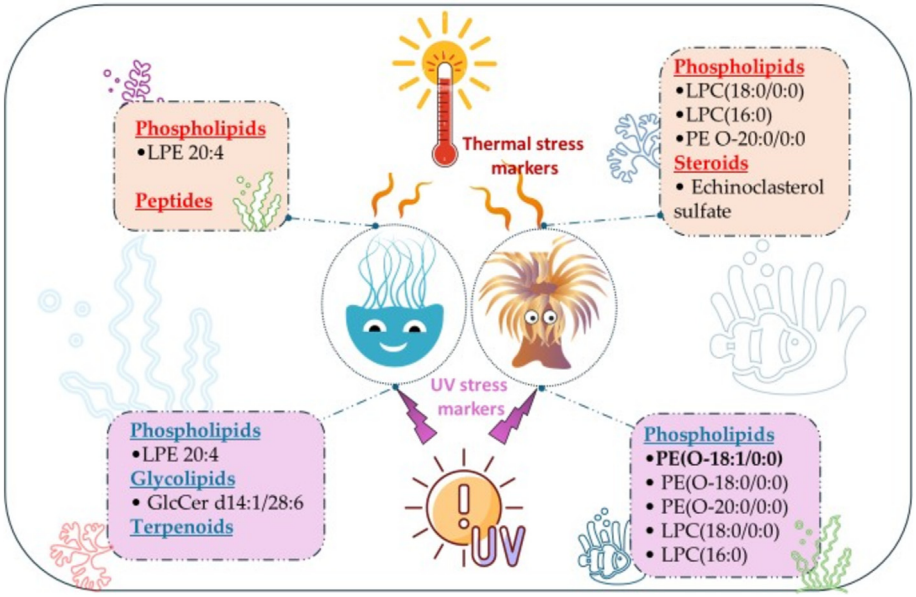

Fig. 9. Diagrammatic sketch summarizing all markers revealed in response to thermal or UV stress in anemones and jellyfish.

While *C. andromeda* is known to contain mainly *Symbiodinium* (formerly clade A), *E. quadricolor* usually harbors different species of *Cladocopium* (formerly clade C) [32,33]. Future studies should therefore include the use of genetic markers such as ITS2 sequencing to detect differences in the Symbiodiniaceae assemblages (for example, following Hume et al. 2019 [70] and LaJeunesse et al. 2018 [71]. Accordingly, this will make it possible to analyze and compare high-throughput sequencing data in a phylogeny-based context [31] and might lead to a better understanding of the variety of marine invertebrate symbionts and how cnidarians adapt to changing environmental conditions.

Conclusion

Metabolomes of the bubble-tip anemone *Entacmaea quadricolor* and the upside-down jellyfish *Cassiopea andromeda* were studied as examples from the family Cnidaria. These two species may have approximate nutritional and symbiotic strategies, and as tropical corals, benefit from photosymbiosis with carbohydrate-producing endosymbiotic algae, which makes them sensitive to environmental changes. Nevertheless, some metabolic changes differed between the two species under stress. This may be due to genetic variation among hosts and/or unicellular symbionts. Additionally, sea anemones have a mutualistic symbiotic relationship with clownfish, which makes them different from jellyfish.

UHPLC-MS coupled with GNPS and chemometrics was used to identify markers for each stress in both marine animals. The two modes of ionization aided in the characterization of different metabolite classes. For example, the negative ionization mode revealed terpenoids and steroid classes, while ceramides and glycolipids were unraveled using the positive ionization mode, highlighting the importance of dual acquisition. Phospholipids represent the major cluster of identified compounds because of their role in maintaining the structural integrity of cell membranes and were detected in both ion modes. PLs served as markers for stress in most MVA models, i.e., LPC (18:0/0:0), LPC (16:0), PE (O-20:0/0:0), PI (18:0/0:0), and PC (O-16:1/0:0) were the most discriminatory markers in anemones, whereas in jellyfish, structural unsaturation played a role in their survival, as represented by LPE (20:4), serving as the phospholipid marker. It should be noted that in jellyfish, levels of unsaturated lipids increase upon thermal and UV stress exposure as a defense mechanism to maintain vital fluidity and viscosity of cell membranes. This is attributed to jellyfish thriving and blooming in warmer environments and phosphonate moieties [72] that contribute to the desaturation process compared to anemones. This can explain why jellyfish were less affected by temperature elevation than anemones. These results confirmed that the observed metabolomic changes were not mediated by unspecific physical contact between the two species, but rather by a dose–response specific stress, i.e., either thermal or UV radiation, as proposed when compared to the control. In the anemone, the thermal stress models showed significant markers, in contrast to the UV stress models, where a significant model was not readily observed. Conversely, the jellyfish thermal stress models did not show significant markers, while UV stress revealed some markers. This aligns with the observed rapid deterioration of jellyfish morphological characteristics upon UV exposure compared to anemones. Moreover, it complies with the observed sudden death of anemones owing to extended temperature elevation, which contrasts with the resilience of jellyfish under the same stress conditions.

In jellyfish, cyclic peptides and terpenoids appear to increase upon thermal stress, but not under UV stress. This is suggestive of a differential response in the case of peptides and terpenoids, and is contrary to phospholipids that were identified in response to both stressors in both organisms. Ceramide phosphonate, sterols, and peptides were the main markers, in addition to PLs, that were revealed among all models of both organisms. However, ceramide markers were exclusively found in jellyfish only after UV exposure. A diagrammatic sketch summarizing all markers revealed in response to thermal or UV stress in anemones and jellyfish is depicted in Fig. 9. In the future, it should be determined whether these chemicals function just as markers for the stress response process in both organisms or contribute towards mitigation against such stressors. Additionally, profiling of other polar low molecular weight chemicals in jellyfish should aid in providing a complete understanding of metabolome changes within that organism, considering that UHPLC-MS targeted mostly the detection of non-polar metabolites, i.e., lipids and terpenes. Identification of the molecular mechanisms underlying these responses

should now follow, based on metabolomics results using other tools such as transcriptomics and proteomics. The sequencing of organisms' microbiomes should also aid in identifying changes in the microbiome consortium inside the animals in response to stress and in detecting strains that could aid in increasing the resilience of these organisms in the future. Likewise, the role of zooxanthellae/Symbiodiniaceae in the stress response mechanisms of these taxa and their interactions within the holobiont, i.e., the exchange of metabolites between host cnidarians and endosymbiotic algae, should be further investigated. Future assessment of Symbiodiniaceae diversity is critical for understanding the symbiotic ecology of corals and the differential responses observed in both marine organisms. The application of genetic markers, such as ITS2 sequencing, following the SymPortal framework [70] to constrain Symbiodiniaceae diversity should therefore be considered in future work. It should be noted that metabolome monitoring represents a holistic pool of all existing organisms inside animals with no dissection of metabolite origin, except in the case of zooxanthellamine; thus, it has yet to be determined by revealing the exact biosynthetic pathway of chemicals in such a complex consortium.

Declaration of competing interest

The authors declare that they have no known competing financial interests or personal relationships that could have appeared to influence the work reported in this paper.

Acknowledgments

Mohamed A. Farag acknowledges the funding received from the Alexander von Humboldt Foundation, Germany. We are grateful to all members of MAREE and the Biolab team at the Leibniz Centre for Tropical Marine Research (ZMT), Germany, especially Silvia Hardenberg, co-head of the Experimental Marine Laboratories, for supporting this study. We appreciate the assistance in setting up the experiment by Elisa Kriege, Hochschule Bremerhaven, Germany.

Appendix A. Supplementary data

Supplementary data to this article can be found online at https://doi.org/10.1016/j.jare.2024.10.007.

References

[1] Karabulut A, McClain M, Rubinstein B, Sabin KZ, McKinney SA, Gibson MC. The architecture and operating mechanism of a cnidarian stinging organelle. Nat Commun 2022;13(1).
[2] Titus BM, Benedict C, Laroche R, Gusmão LC, Van Deusen V, Chiodo T, et al. Phylogenetic relationships among the clownfish-hosting sea anemones. Mol Phylogenet Evol 2019;139:106526.
[3] Mebs D. Anemonefish symbiosis: vulnerability and resistance of fish to the toxin of the sea anemone. Toxicon: Official Journal of the International Society on Toxinology 1994;32(9):1059–68.
[4] Mebs D. Chemical biology of the mutualistic relationships of sea anemones with fish and crustaceans. Toxicon: Official Journal of the International Society on Toxinology 2009;54(8):1071–4.
[5] Hoepner CM, Fobert EK, Abbott CA, Da Silva KB. No place like home: Can omics uncover the secret behind the sea anemone and anemonefish symbiotic relationship? Evolution, Development and Ecology of Anemonefishes. CRC Press; 2022. p. 197–208.
[6] Hoepner CM, Stewart ZK, Qiao R, Fobert EK, Prentis PJ, Colella A, et al. Proteotransciptomics of the Most Popular Host Sea Anemone *Entacmaea quadricolor* Reveals Not All Toxin Genes Expressed by Tentacles Are Recruited into Its Venom Arsenal. Toxins 2024;16(2):85.
[7] Al-Hammady MAMM, Silva TF, Hussein HNM, Saxena G, Modolo LV, Belasy MBI, et al. How do algae endosymbionts mediate for their coral host fitness under heat stress? A comprehensive mechanistic overview. Algal Res 2022;67:102850.
[8] Janzen S, Narvaez L, O'Connor J. Technical Report Coral Bleaching in the Great Barrier Reef. 2021.
[9] Hayashi K, Reimer JD. Five-year study on the bleaching of anemonefish-hosting anemones (Cnidaria: Anthozoa: Actiniaria) in subtropical Okinawajima Island. Reg Stud Mar Sci 2020;35:101240.
[10] Farag MA, Meyer A, Ali SE, Salem MA, Giavalisco P, Westphal H, et al. Comparative Metabolomics Approach Detects Stress-Specific Responses during Coral Bleaching in Soft Corals. J Proteome Res 2018;17(6):2060–71.
[11] Wissmann SM. The effects of elevated ultraviolet B radiation and elevated water temperature on the loss of zooxanthellae from *Aiptasia pallida*. Transactions of the Kansas Academy of Science. 2003. 106 (1). 92-8, 7.
[12] Pontasch S, Hill R, Deschaseaux E, Fisher PL, Davy SK, Scott A. Photochemical efficiency and antioxidant capacity in relation to *Symbiodinium* genotype and host phenotype in a symbiotic cnidarian. Mar Ecol Prog Ser 2014;516:195–208.
[13] Moya A, Ganot P, Furla P, Sabourault C. The transcriptomic response to thermal stress is immediate, transient and potentiated by ultraviolet radiation in the sea anemone *Anemonia viridis*. Mol Ecol 2012;21(5):1158–74.
[14] Prasade A, Nagale P, Apte D. Cassiopea andromeda (Forsskål, 1775) in the Gulf of Kutch, India: initial discovery of the scyphistoma, and a record of the medusa in nearly a century. Marine Biodiversity Records. 2016. 9(1).
[15] De Domenico S, De Rinaldis G, Paulmery M, Piraino S, Leone A. Barrel Jellyfish (Rhizostoma pulmo) as Source of Antioxidant Peptides. Mar Drugs 2019;17(2):134.
[16] Purcell J. Climate effects on formation of jellyfish and ctenophore blooms: A review. J Mar Biol Assoc U K 2005;85:461–76.
[17] Pauly D, Graham W, Libralato S, Morissette L, Palomares MLD. Jellyfish Blooms: Causes, Consequences, and Recent Advances. Hydrobiologia 2008;616:67–85.
[18] Deidun A. Back with a bang – an unexpected massive bloom of Cassiopea andromeda (Forskaal, 1775) in the Maltese Islands, nine years after its first appearance. BioInvasions Records 2018;7:399–404.
[19] Rowe CE, Keable SJ, Ahyong ST, Figueira WF. Physiological responses of the upside-down jellyfish, *Cassiopea* (Cnidaria: Scyphozoa: Cassiopeidae) to temperature and implications for their range expansion along the east coast of Australia. J Exp Mar Biol Ecol 2022;554:151765.
[20] Klein SG, Pitt KA, Carroll AR. Surviving but not thriving: inconsistent responses of zooxanthellate jellyfish polyps to ocean warming and future UV-B scenarios. Sci Rep 2016;6(1):28859.
[21] Aljbour SM, Alves RN, Agustí S. Aerobic respiration, biochemical composition, and glycolytic responses to ultraviolet radiation in jellyfish *Cassiopea* sp.. Front Mar Sci 2023;9.
[22] Hillyer KE, Tumanov S, Villas-Bôas S, Davy SK. Metabolite profiling of symbiont and host during thermal stress and bleaching in a model cnidarian-dinoflagellate symbiosis. J Exp Biol 2015;219(4):516–27.
[23] Lohr KE, Khattri RB, Guingab-Cagmat J, Camp EF, Merritt ME, Garrett TJ, et al. Metabolomic profiles differ among unique genotypes of a threatened Caribbean coral. Sci Rep 2019;9(1).
[24] Matthews JL, Oakley CA, Lutz A, Hillyer KE, Roessner U, Grossman AR, et al. Partner switching and metabolic flux in a model cnidarian–dinoflagellate symbiosis. Proc R Soc B Biol Sci 2018;285(1892):20182336.
[25] Rosset SL, Oakley CA, Ferrier-Pagès C, Suggett DJ, Weis VM, Davy SK. The molecular language of the cnidarian–dinoflagellate symbiosis. Trends Microbiol 2021;29(4):320–33.
[26] Williams A, Chiles EN, Conetta D, Pathmanathan JS, Cleves PA, Putnam HM, et al. Metabolomic shifts associated with heat stress in coral holobionts. Sci Adv 2021;7(1):eabd4210.
[27] Mariottini G, Grice I. Antimicrobials from Cnidarians. A New Perspective for Anti-Infective Therapy? Mar Drugs 2016;14(3):48.
[28] De Rinaldis G, Paulmery M, Gallo A, Bleve G, Piraino S, Leone A. Jellyfish proteins as bioactive compounds in novel foods. 2018.
[29] Riccio G, Martinez KA, Martín J, Reyes F, D'Ambra I, Lauritano C. Jellyfish as an Alternative Source of Bioactive Antiproliferative Compounds. Mar Drugs 2022;20(6):350.
[30] Zhang H, Zou J, Yan X, Chen J, Cao X, Wu J, et al. Marine-Derived Macrolides 1990–2020: An Overview of Chemical and Biological Diversity. Mar Drugs 2021;19(4):180.
[31] Arif C, Daniels C, Bayer T, Banguera-Hinestroza E, Barbrook A, Howe CJ, et al. Assessing *Symbiodinium* diversity in scleractinian corals via next-generation sequencing-based genotyping of the ITS2 rDNA region. Mol Ecol 2014;23(17):4418–33.
[32] Arossa S, Barozzi A, Callegari M, Klein SG, Parry AJ, Hung S-H, et al. The internal microenvironment of the symbiotic jellyfish *cassiopea* sp. from the red Sea. Frontiers in Marine Science. 2021. 8.
[33] Lampert KP, Bürger P, Striewski S, Tollrian R. Lack of association between color morphs of the Jellyfish *Cassiopea andromeda* and zooxanthella clade. Mar Ecol 2012;33(3):364–9.
[34] Farag MA, Al-Mahdy DA, Meyer A, Westphal H, Wessjohann LA. Metabolomics reveals biotic and abiotic elicitor effects on the soft coral Sarcophyton ehrenbergi terpenoid content. Sci Rep 2017;7(1):648.
[35] Olivon F, Grelier G, Roussi F, Litaudon M, Touboul D. MZmine 2 Data-Preprocessing To Enhance Molecular Networking Reliability. Anal Chem 2017;89.

[36] Dührkop K, Nothias L-F, Fleischauer M, Reher R, Ludwig M, Hoffmann MA, et al. Systematic classification of unknown metabolites using high-resolution fragmentation mass spectra. Nat Biotechnol 2021;39(4):462–71.
[37] Schmid R, Petras D, Nothias L-F, Wang M, Aron AT, Jagels A, et al. Ion identity molecular networking for mass spectrometry-based metabolomics in the GNPS environment. Nat Commun 2021;12(1).
[38] Jacob H, Springer K, Belter L, Kunzmann A. Symbiodiniaceae *in* and *ex hospite* have differential physiological responses under different heat stress scenarios. Mar Biol Res 2023;19(2–3):108–20.
[39] Körber T, Sitz T, Abdalla M, Mühling K, Rohn S. LC-ESI-MS/MS Analysis of Sulfolipids and Galactolipids in Green and Red Lettuce (Lactuca sativa L.) as Influenced by Sulfur Nutrition. Int J Mol Sci 2023.
[40] Hartmann AC, Petras D, Quinn RA, Protsyuk I, Archer FI, Ransome E, et al. Meta-mass shift chemical profiling of metabolomes from coral reefs. Proc Natl Acad Sci 2017;114(44):11685–90.
[41] Korinek M, Tsai Y-H, El-Shazly M, Lai K-H, Backlund A, Wu S-F, et al. Anti-allergic Hydroxy Fatty Acids from Typhonium blumei Explored through ChemGPS-NP. Front Pharmacol 2017;8.
[42] Ma Y, Yu H, Xing R, Liu S, Li P. Lipid-lowering activity and mechanism of peptides from jellyfish Nemopilema nomurai. J Funct Foods 2023;101:105421.
[43] Rey F, Melo T, Lopes D, Couto D, Marques F, Domingues MR. Applications of lipidomics in marine organisms: progress, challenges and future perspectives. Molecular Omics 2022;18(5):357–86.
[44] Pi J, Wu X, Feng Y. Fragmentation patterns of five types of phospholipids by ultra-high-performance liquid chromatography electrospray ionization quadrupole time-of-flight tandem mass spectrometry. Anal Methods 2016;8(6):1319–32.
[45] Leblond JD, Khadka M, Duong L, Dahmen JL. Squishy lipids: Temperature effects on the betaine and galactolipid profiles of a C₁₈/C₁₈peridinin-containing dinoflagellate, Symbiodinium microadriaticum(Dinophyceae), isolated from the mangrove jellyfish, Cassiopea xamachan. Phycol Res 2015;63(3):219–30.
[46] Kariotoglou DM, Mastronicolis SK. Sphingophosphonolipids, phospholipids, and fatty acids from aegean jellyfish Aurelia aurita. Lipids 2001;36(11):1255–64.
[47] Cunha SA, Pintado ME. Bioactive peptides derived from marine sources: Biological and functional properties. Trends Food Sci Technol 2022;119:348–70.
[48] Reinicke J, Kitatani R, Masoud SS, Galbraith KK, Yoshida W, Igarashi A, et al. Isolation, Structure Determination, and Synthesis of Cyclic Tetraglutamic Acids from Box Jellyfish Species Alatina alata and Chironex yamaguchii. Molecules 2020;25(4):883.
[49] Dahiya R, Gautam H. Toward the Synthesis and Biological Screening of a Cyclotetrapeptide from Marine Bacteria. Mar Drugs 2010;9(1):71–81.
[50] Núñez-Pons L, Shilling A, Verde C, Baker BJ, Giordano D. Marine Terpenoids from Polar Latitudes and Their Potential Applications in Biotechnology. Mar Drugs 2020;18(8):401.
[51] Kim S-K, Li Y-X. Chapter 26 - Biological Activities and Health Effects of Terpenoids from Marine Fungi. In: Kim S–K, editor. Advances in Food and Nutrition Research. 65: Academic Press; 2012. p. 409–13.
[52] Gross H, König GM. Terpenoids from Marine Organisms: Unique Structures and their Pharmacological Potential. Phytochem Rev 2006;5(1):115–41.
[53] Gordon BR, Leggat W. Symbiodinium—Invertebrate Symbioses and the Role of Metabolomics. Mar Drugs 2010;8(10):2546–68.
[54] Farag M, Meyer A, Ezz S. Bleaching effect in Sarcophyton spp. soft corals—is there a correlation to their diterpene content? Environ Sci Pollut Res 2021;28:1–9.
[55] Georgantea P, Ioannou E, Vagias C, Roussis V. Bisabolane and chamigrane sesquiterpenes from the soft coral Pseudopterogorgia rigida. Phytochem Lett 2014;8.
[56] Duh CY, Wang S-k, Brassicolene W-L. a novel cytotoxic diterpenoid from the Formosan soft coral Nephthea brassica. Tetrahedron Lett 2000;41:1401–3.
[57] Mariottini G, Pane L. Cytotoxic and Cytolytic Cnidarian Venoms. A Review on Health Implications and Possible Therapeutic Applications Toxins 2013;6:108–51.
[58] Al-Mutlaq KF, Standley LJ, Simoneit BRT. Composition and sources of extractable organic matter from a sediment core in Lake Kivu. East African rift valley Applied Geochemistry 2008;23(5):1023–40.
[59] Das R, Rauf A, Mitra S, Emran TB, Hossain MJ, Khan Z, et al. Therapeutic potential of marine macrolides: An overview from 1990 to 2022. Chem Biol Interact 2022;365:110072.
[60] Liu T-F, Lu X, Tang H, Zhang M-M, Wang P, Sun P, et al. 3β,5α,6β-Oxygenated sterols from the South China Sea gorgonian Muriceopsis flavida and their tumor cell growth inhibitory activity and apoptosis-inducing function. Steroids 2013;78(1):108–14.
[61] Harshfield E, Koulman A, Ziemek D, Marney L, Fauman E, Paul D, et al. An Unbiased Lipid Phenotyping Approach To Study the Genetic Determinants of Lipids and Their Association with Coronary Heart Disease Risk Factors. J Proteome Res 2019;18:2397–410.
[62] Imbs AB, Dang LPT, Nguyen KB. Comparative lipidomic analysis of phospholipids of hydrocorals and corals from tropical and cold-water regions. PLoS One 2019;14(4):e0215759.
[63] Chen H-K, Song S-N, Wang L-H, Mayfield AB, Chen Y-J, Chen W-N-U, et al. A Compartmental Comparison of Major Lipid Species in a Coral-Symbiodinium Endosymbiosis: Evidence that the Coral Host Regulates Lipogenesis of Its Cytosolic Lipid Bodies. PLoS One 2015;10(7):e0132519.
[64] Lima MS, Hamerski L, Silva TA, da Cruz MLR, Varasteh T, Tschoeke DA, et al. Insights on the biochemical and cellular changes induced by heat stress in the Cladocopium isolated from coral Mussismilia braziliensis. Front Microbiol 2022;13.
[65] Sikorskaya TV. Coral Lipidome: Molecular Species of Phospholipids, Glycolipids, Betaine Lipids, and Sphingophosphonolipids. Marine Drugs [Internet]. 2023. 21(6).
[66] Farag MA, Kabbash EM, Mediani A, Döll S, Esatbeyoglu T, Afifi SM. Comparative metabolite fingerprinting of four different cinnamon species analyzed via UPLC–MS and GC–MS and chemometric tools. Molecules 2022;27(9):2935.
[67] Ernst R, Ejsing CS, Antonny B. Homeoviscous Adaptation and the Regulation of Membrane Lipids. J Mol Biol 2016;428(24, Part A):4776–91.
[68] Stien D, Suzuki M, Rodrigues AMS, Yvin M, Clergeaud F, Thorel E, et al. A unique approach to monitor stress in coral exposed to emerging pollutants. Sci Rep 2020;10(1).
[69] Mendoza-Porras O, Rusu AG, Stratford C, Wade NM. Rapid detection of heat stress biomarkers in Atlantic salmon (Salmo salar) liver using targeted proteomics. Aquaculture, Fish and Fisheries 2024;4(1):1–12.
[70] Hume BCC, Smith EG, Ziegler M, Warrington HJM, Burt JA, LaJeunesse TC, et al. SymPortal: A novel analytical framework and platform for coral algal symbiont next-generation sequencing *ITS2* profiling. Mol Ecol Resour 2019;19(4):1063–80.
[71] LaJeunesse TC, Parkinson JE, Gabrielson PW, Jeong HJ, Reimer JD, Voolstra CR, et al. Systematic revision of Symbiodiniaceae highlights the antiquity and diversity of coral endosymbionts. Curr Biol 2018;28(16):2570. 2580.e6.
[72] Paweł K. Phosphonates: Their Natural Occurrence and Physiological Role. In: David GC, Maja Dutour S, Božana Č, Helga Füredi M, editors. Contemporary Topics about Phosphorus in Biology and Materials. Rijeka: IntechOpen; 2019. Ch. 6.